Ab initio calculations of NMR satellite data for 3*d* impurities in Cu

B. Drittler
Institut für Festkörperforschung, Kernforschungsanlage Jülich, D-5170 Jülich, Federal Republic of Germany

H. Ebert
Siemens AG, ZFE TPH11, Paul-Gossen-Strasse 100, D-8520 Erlangen, Federal Republic of Germany

R. Zeller and P. H. Dederichs
Institut für Festkörperforschung Kernforschungsanlage Jülich, D-5170 Jülich, Federal Republic of Germany
(Received 28 September 1988)

We report about self-consistent calculations for 3*d* impurities in Cu which are based on density functional theory and the Korringa-Kohn-Rostoker- (KKR) Green's function method. In particular, we calculate the magnetization disturbance and the hyperfine fields for six shells of Cu atoms around the impurities. The results are compared with measured Knight-shift satellite positions. In practically all cases we get good agreement with the reported satellite positions. As a function of the impurity atomic number we obtain very simple and characteristic trends for the hyperfine fields of the first six shells. In some cases this allows us to correct for erroneous assignments of the experimentally observed satellite peaks to the different shells around the impurity.

I. INTRODUCTION

3*d* impurities in noble metals are the classical examples of magnetic impurities, showing a Kondo behavior at low temperature. There are numerous experimental and theoretical investigations of these systems in the literature. Especially detailed information has been obtained by nuclear magnetic studies of Cu alloys. In particular the Slichter group (see the references given below) has performed very extensive nuclear magnetic resonance (NMR) satellite measurements of all 3*d* impurities in Cu aiming at revealing the magnetization distribution around the impurities. For Cr, Mn, and Fe up to five satellite peaks have been observed and assigned to the Cu atoms of different shells around the impurities. Thus a wealth of information exists about the magnetization of the nearby Cu atoms.

The relation of these data to the electronic structure and the local moments of the impurities is less clear. The most ambitious effort in this direction is the work of Cohen and Slichter.[1] These authors performed jellium-type model calculations in which they fitted the impurity potential to the experimental information about the impurity susceptibility and the host satellite data. In general, a consistent picture evolved from the calculation about the behavior of these impurities. The present work is aimed at putting such calculations on a sounder ground. Some years ago we were able to calculate the electronic structure and the magnetic moments of 3*d* impurities in Cu (Refs. 2 and 3) on the *ab initio* basis using density functional theory in the local-density approximation. The calculated moments for Cu and Ag alloys are in quite good agreement with the experimental data. Certainly this approach is not perfect since, for example, the Kondo effect cannot be described in the local-density approximation. Nevertheless the agreement of the experimental data shows that many aspects of these systems can be successfully described by the local-density approximation. In this paper we extend these calculations and evaluate the charge and magnetization perturbations for six shells of Cu atoms around the 3*d* impurities. Our central interest is, however, focused on the hyperfine fields of these Cu atoms. The results of our parameter-free calculations are generally in good agreement with the experimental NMR data. In some cases, however, discrepancies occur with respect to the assignment of the satellite peaks to the different shells around the impurities. Our results give particularly clear and characteristic trends for the hyperfine fields of the first six-shell atoms, which in some cases allows us to correct for the obviously erroneous assignments of the experimental peaks. This clearly shows the strength of first-principles calculations where no fitting to the experimental data is necessary.

II. THEORETICAL METHODS AND EVALUATION OF THE DATA

To permit a detailed discussion of the influence of impurities dissolved in Cu on the magnetic properties of the surrounding Cu atoms, we have performed calculations of the electronic structure for such systems. A short description of these calculations, which correspond to the experimental situation of zero temperature and vanishing external field, is given in the next subsection. Although the actual experimental situation differs strongly from this hypothetical situation, it is possible to deduce from the experimental NMR satellite data information that can be directly compared to the hyperfine fields emerging from our calculations. The way this can be done is described in Sec. II B.

A. Electronic structure calculation

Our calculational method is based on the multiple scattering theory. The Green's function of the electrons, which are multiply scattered by a collection of nonoverlapping muffin-tin potentials centered at positions $\mathbf{R}^n$, is expanded into eigensolutions of these spherically symmetric local potentials:[2,3]

$$G(\mathbf{r}+\mathbf{R}^n,\mathbf{r}'+\mathbf{R}^{n'};E)=\delta_{nn'}\sqrt{E}\sum_L Y_L(\hat{\mathbf{r}})R_l^n(r_<,E)H_l^n(r_>,E)Y_L(\hat{\mathbf{r}}') + \sum_{L,L'} Y_L(\hat{\mathbf{r}})R_l^n(r,E)G_{LL'}^{nn'}(E)R_{l'}^{n'}(r',E)Y_{L'}(\hat{\mathbf{r}}') , \quad (1)$$

in Rydberg atomic units. The position vectors $\mathbf{r},\mathbf{r}'$ are restricted to the Wigner-Seitz cell and $r_<$ and $r_>$ are the smaller and larger of $r=|\mathbf{r}|$ and $r'=|\mathbf{r}'|$. The subscript $L=(l,m)$ denotes angular momentum quantum numbers and Y_L are real spherical harmonics. The irregular H_l^n and regular R_l^n solutions of the radial Schrödinger equation for the nth muffin-tin potential at energy E are defined by their asymptotic behavior outside the muffin-tin sphere of radius R_{MT} ($r \geq R_{\mathrm{MT}}$):

$$H_l^n(r,E)=h_l(r\sqrt{E}) ,$$
$$R_l^n(r,E)=j_l(r\sqrt{E})+\sqrt{E}\,t_l^n(E)h_l(r\sqrt{E}) , \quad (2)$$

where j_l and h_l are the spherical Bessel and Hankel functions and t_l^n the usual t matrix for the nth single potential.

The information about the multiple scattering between muffin tins is contained in the structural Green's function matrix $G_{LL'}^{nn'}$. It can be related to its counterpart for the host crystal by an algebraic Dyson equation:

$$G_{LL'}^{nn'}(E)=G_{LL'}^{0nn'}(E) + \sum_{n'',L''} G_{LL''}^{0nn''}(E)[t_{l''}^{n''}(E)-t_{l''}^{0n''}(E)] \times G_{L''L'}^{n''n'}(E) , \quad (3)$$

where the 0 superscript refers to the host. This equation describes correctly and in a very efficient way the embedding of the defect into the ideal crystal. In our calculation the angular momentum expansion in the Green's functions includes s, p, d, and f electrons, and the perturbation of the host atoms is considered to be extended up to six shells, including 86 Cu atoms. The resulting matrices have the rank 1.392×1.392 and are decomposed into their irreducible parts by group theory. The largest matrices involved then have the size 100×100.

All potentials, i.e., the host potential, the impurity potential and the perturbed potentials of the Cu atoms in the first six shells, are determined self-consistently in the framework of density-functional theory. Exchange and correlation effects are included through the local spin-density approximation of von Barth and Hedin[4] with the constants as given by Moruzzi *et al.*[5] The necessary charge and magnetization densities are obtained for the valence states by complex energy integration of the Green's function up to the Fermi energy.[6] The core electrons can relax and are recalculated in each iteration. The Green's function $G_{LL''}^{0nn'}(E)$ of the host is obtained from a self-consistent band-structure calculation for pure Cu. For more details about the calculational method we refer to Refs. 2 and 3. The introduction of the host Green's functions guarantees that all band-structure effects are properly accounted for. The major approximations in our calculation are (1) the local-density approximation for the exchange and correlation, (2) the atomic-sphere approximation for the potentials, and (3) the neglect of lattice relaxations around the impurity.

The leading contribution to the hyperfine field H is given by the Fermi-contact interaction and is determined by the magnetization density $m(\mathbf{R}^n)$ at the nuclear position $\mathbf{R}^n$ of the considered atom:

$$H_n=\frac{8\pi}{3}\mu_B m(\mathbf{R}^n) . \quad (4)$$

There exist additional small orbital and dipolar contributions which are neglected in the following. Relativistic corrections to the Fermi-contact interaction are relatively small in the $3d$ series[7] and are also neglected. In our calculations we determine the hyperfine fields H_n for the Cu neighbors in the first six shells ($n=1,\ldots,6$) around the impurity, i.e., we just calculate the magnetization densities at the nuclear positions $\mathbf{R}^n$.

B. Comparison with experiments

Experimentally, the influence of impurities on the magnetic properties of the surrounding Cu atoms is studied by determining the additional hyperfine fields $\Delta H_n(T)$, which an external field B_{ext} induces on the nth-shell Cu atoms relative to the unperturbed bulk atoms. These additional hyperfine fields ΔH_n give rise to the NMR satellites and are found to be proportional to the external field B_{ext}:

$$\Delta H_n(T)=\Delta K_n(T)B_{\mathrm{ext}} , \quad (5)$$

where ΔK_n is the additional Knight shift of the satellite n. In the Fermi contact approximation $\Delta H_n(T)$ is given by the temperature-dependent change $\Delta m(\mathbf{R}^n,T)$ of the magnetization at the atomic site $\mathbf{R}^n$ being induced by the external field

$$\Delta H_n(T)=\frac{8\pi}{3}\mu_B\Delta m(\mathbf{R}_n,T) . \quad (6)$$

Experimentally it has been found that $\Delta m(\mathbf{R}_n,T)$ can be split into the spin susceptibility $\chi(T)$ of the impurity and a temperature-independent spatial shape function $f(\mathbf{R}^n)$:

$$\Delta H_n(T)=\frac{4\pi}{3}\mu_B\chi(T)B_{\text{ext}}f(\mathbf{R}^n)=\Delta K_n(T)B_{\text{ext}} \ . \quad (7)$$

Physically this means that the magnetization cloud around the impurity follows instantaneously the rotation of the impurity moment in the external field.

The temperature independence of the shape function $f(\mathbf{R}^n)$ provides the opportunity to compare the results of our calculations with the experiment. In the calculation we assume that the direction of the moment is fixed. This corresponds to the high-field low-temperature limit where all impurity moments are fully aligned in the magnetic field. Then the hyperfine fields are given by (4) and are independent of the external fields. Practical experimental conditions are different from this and corresponds to the high-temperature low-field limit, where the impurity moments more or less freely rotate. Accordingly the spin susceptibility $\chi(T)$ of the impurity normally obeys a Curie-Weiss law,

$$\chi(T)=\frac{p_{\text{eff}}^2}{3k_B(T+T_K)} \ , \quad (8)$$

with an effective moment $p_{\text{eff}}=2\mu_B\sqrt{S(S+1)}$ where S is the total spin of the impurity. T_K denotes the Kondo temperature. Since the polarization cloud is assumed to rotate together with the impurity the effective moment p_{eff} refers to the total moment $M_t=2S$ of the impurity including the host contribution. Contrary to the high-temperature limit [(5)–(7)] the calculated ground-state values of the hyperfine fields H_n are given by (4):

$$H_n=\frac{8\pi}{3}\mu_B m(\mathbf{R}^n,T=0)=\frac{8\pi}{3}\mu_B M_t f(\mathbf{R}^n) \ . \quad (9)$$

This simple relation between the ground-state fields H_n and the high-temperature shifts $\Delta H_n(T)$ allows us to extract from the experiment a hypothetical experimental value H_n^{expt} for the ground-state field H_n, if both the Knight shift $\Delta K_n(T)$ and the susceptibility $\chi(T)$ are known. By solving Eq. (7) with respect to $f(\mathbf{R}^n)$ and inserting this into (9) one obtains

$$H_n^{\text{expt}}=2\mu_B S\Delta K_n(T)/\chi(T) \ . \quad (10)$$

Thus if both $\Delta K_n(T)$ and $\chi(T)$ have been measured at a certain reference temperature T_{expt}, we can estimate from this a hypothetical ground-state field H_n^{expt} where we use for S the experimental or calculated value for the total moment $M_t=2S$. If the susceptibility $\chi(T)$ satisfies a Curie-Weiss law (8) we can rewrite Eq. (10) as

$$H_n^{\text{expt}}=\frac{3k_B}{2\mu_B(S+1)}\Delta K_n(T)(T+T_K) \ . \quad (11)$$

The hyperfine fields H_n deduced in this way from the Knight shifts $K_n(T)$ and the impurity spin S are denoted in the following as $H_n^{\text{exp}}(A)$ ("method A") whereas the above fields (10) estimated from $\Delta K_n(T)$ and $\chi(T)$ are referred to as $H_n^{\text{expt}}(B)$ ("method B").

III. RESULTS AND DISCUSSION

Table I gives a summary of the calculated local moments for $3d$ impurities in Cu. Given are the impurity moment M_0 and the moments M_n induced on the Cu atoms in the nth shell around the impurity (for the first six shells). Also the total moments M_t as the sum of the impurity moments and all induced moments are given. The calculated impurity moments are in quite good agreement with the experimental data and will not be discussed here (see Refs. 2 and 3 for details).

The moments $M_1,\ldots,M_6$ of the Cu atoms around the impurity show Friedel-like oscillations with small positive and negative contributions more or less canceling each other. The total moment M_t is therefore not very different from the local impurity moment M_0. Somewhat larger deviations of about 0.2 to $0.3\mu_B$ occur for Mn, Cr, and V. Most of this enhancement can be traced to the

TABLE I. Local moments for $3d$ impurities in Cu. The local moments M_0 in the impurity Wigner-Seitz sphere and the induced moments $M_1,\ldots,M_6$ of Cu atoms in the first six shells around the impurity are given. M_t is the total moment including host contributions. $M_{1s},\ldots,M_{6s}$ are the partial contributions to the local moments on the Cu atoms due to s electrons alone.

	V	Cr	Mn	Fe	Co
M_0	1.10	2.99	3.40	2.51	0.89
M_1	+0.0167	+0.0310	+0.0226	+0.0084	−0.0001
M_2	−0.0028	−0.0079	−0.0090	−0.0072	−0.0022
M_3	+0.0015	+0.0019	+0.0003	−0.0012	−0.0009
M_4	−0.0010	−0.0021	−0.0022	−0.0015	−0.0004
M_5	−0.0002	−0.0005	−0.0005	−0.0004	−0.0001
M_6	−0.0014	−0.0022	−0.0012	−0.0000	+0.0004
M_t	1.29	3.30	3.58	2.51	0.85
M_{1s}	−0.0010	−0.0041	−0.0065	−0.0057	−0.0022
M_{2s}	−0.0014	−0.0009	+0.0017	+0.0030	+0.0017
M_{3s}	+0.0003	+0.0006	+0.0005	+0.0002	+0.0000
M_{4s}	−0.0006	−0.0017	−0.0021	−0.0017	−0.0006
M_{5s}	−0.0001	−0.0002	+0.0000	+0.0001	+0.0001
M_{6s}	−0.0003	−0.0003	+0.0000	+0.0002	+0.0001

TABLE II. Theoretical (H_n^{th}) and experimental [$H_n^{expt}(A)$,$H_n^{expt}(B)$] hyperfine fields for Cu-V (units: kG). H_n is the hyperfine field in the nth shell around the impurity. Also given are the conventional peak nomenclature and the assignment of these peaks to the various shells as found in the cited literature. Question marks indicate that the experimental assignment is uncertain.

Shell	H_n^{th}	$H_n^{expt}(A)$	$H_n^{expt}(B)$	$\Delta K_n/K$[a]	Peak	Expt. assign.
1	−9.1					
2	−8.0	−6.0	−11.2	−0.658±0.015	*G*	2 (or 4?)
3	+1.8	+1.8	+3.4	+0.2±0.1	*C*	3?
4	−3.6					
5	−0.9					
6	−1.5					

[a]Reference 9.

moments M_1 of the first-shell Cu atoms. This trend is most easily described in a jellium model.[1,8] In the series Co, . . . , V the first minimum of the Friedel-like magnetization oscillation shifts from about 0.75 of the nearest-neighbor distance to the nearest-neighbor distance itself. As a consequence for Co and nearly so for Fe the positive and negative contributions within the nearest-neighbor cell cancel each other whereas for Mn, Cr, and V the positive contributions dominate the negative ones.

The hyperfine fields H_n are determined by the magnetization density at the nuclear position $\mathbf{R}^n$. Due to the core oscillations of the s-wave functions this is a rather complicated quantity which is not in any direct way related to the average moment M_n in the nth cell. The valence contributions of the hyperfine fields are, however, in a good approximation proportional to the average moment M_{ns} of the valence s electrons.[7] Therefore we have listed in Table I also the contributions M_{ns} to the moment M_n arising from the local s electrons alone.

The calculated hyperfine fields for the first four shells around the impurity are summarized in Fig. 1 and in detail in Tables II–VI for the individual systems. The calculations show that the core polarization effect is not important since the Cu atoms have no well-defined local moments. The core typically gives a contribution of 6–8 % to the total hyperfine fields for the first shell and even smaller contributions for the other ones. Therefore the valence contributions dominate and the fields correlate well[7] with the calculated s moments of Table I. Consequently the hyperfine fields are transferred fields, arising from the scattering of the host electrons at the strongly exchange-splitted potential of the impurity. The calculations show that the exchange enhancement of the Cu atoms, though fully included in the calculation, is not of major importance. Even a calculation where only the impurity potential is perturbed and taken from a self-consistent calculation, gives already qualitatively the correct behavior for the magnetization density and the hyperfine fields. For this reason density-functional theory should be able to predict quite reliably hyperfine fields. This is different to the situation in ferromagnetic alloys[7] where the intra-atomic s-d polarization, because of the core polarization effect, is of strong importance and causes some problems for local-density functional calculations.

The hyperfine fields H_n for the different shells show some special trends. The field of the first shell is normally the biggest one and strongly negative, whereas the field of the second shell is large and positive for Co, Fe, and Mn and then, however, changes sign for Cr and V. The field of the third shell is for all impurities quite moderate and positive and the fourth one astonishingly large and negative. The strong parabolic variation (see Fig. 1) of the first-shell hyperfine field essentially reflects the variation of the local moment of the impurities, since one would expect that the induced magnetization at the first-

TABLE III. Theoretical (H_n^{th}) and experimental [H_n^{expt},$H_n^{expt}(A)$] hyperfine fields for Cu-Cr (units: kG).

Shell	H_n^{th}	H_n^{expt} [a]	$H_n^{expt}(A)$	$\Delta K_n/K$[b]	Peak	Expt. assign.
1	−31.1		−34.2±1.8	−5.57±0.30	*A*	1
2	−3.7					
3	+3.3	+3.0±0.2	+4.2±0.1	+0.68±0.02	*M*	3
4	−10.4	−6.3±0.3	−8.4±0.2	−1.36±0.04	*B*	4
5	−1.4		−2.6±1	−0.42±0.02	*C*	5?
6	−1.9					
≥7		2.0+0.1	2.7±0.1	0.436±0.01	*N*	7?
≥7		1.2±0.05	1.6±0.1	0.26±0.02	*P*	2?

[a]Reference 12.
[b]Reference 11.

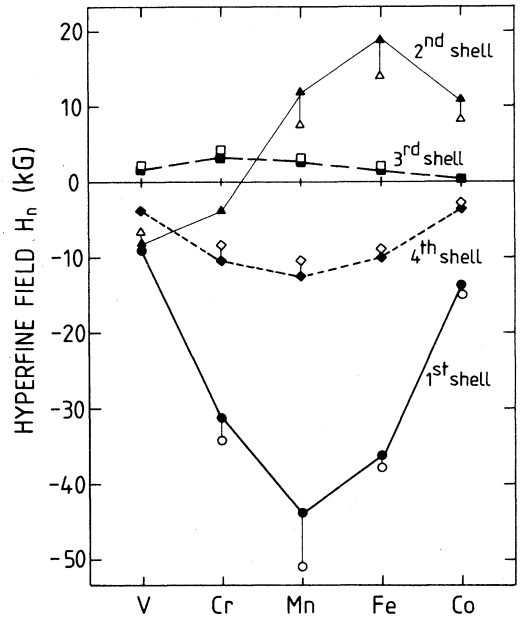

FIG. 1. Hyperfine fields for the different shell atoms around the impurity. The filled symbols (●,▲,■,◆) refer to the calculated values, the open symbols (○,△,□◇) to the corresponding experimental data, with the assignments as made in the present paper. For clarity only the first four shells are shown.

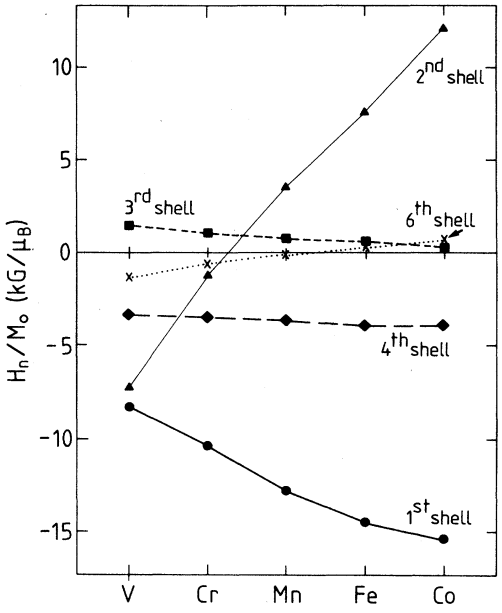

FIG. 2. The ratio H_n/M_0 of the hyperfine field H_n of the nth shell over the impurity moment M_0 for the first six shells around the impurity. The values for the fifth shell are similar but slightly smaller than the values for the sixth one.

shell sites is proportional to the impurity moment but opposite in sign. For these reasons we have plotted in Fig. 2 the ratio of the hyperfine field H_n divided by the impurity moment M_0. Compared to Fig. 1 a pronounced regularity of the data becomes obvious. The ratios for the different shells all lie on approximately straight lines. In the sequence V to Co the ratios for the first shell are slightly decreasing, the second ones are strongly increasing, and the third and fourth ones are more or less constant. The hyperfine fields of the fifth and sixth shell are very small and change sign in the middle of the 3*d* series, similarly to the second shell. Figure 2 shows even more clearly than Fig. 1 that the hyperfine fields H_n of the same shell are strongly correlated for different impurities. For instance, even if we would not have calculated the Cu-Fe system but only the neighboring elements Mn and Co one could easily estimate the ratio H_n/M_0 for Fe by interpolating the values of the neighboring elements, without making any significant error. The hyperfine fields H_n could then be obtained by multiplying with the local moment of Fe which is well known. Thus Fig. 2 demonstrates that it is practically impossible to make errors in the calculation for a specific impurity, say Fe, if the calculated values for the neighboring impurities are correct and agree with the experiment. We will use this argument later on, especially in the case of Fe, to correct some erroneous assignments of satellite peaks.

We will now discuss the individual impurities separately and compare the calculated field H_n in connection with the experimental data. In Tables II–VI, H_n^{th} denote the

TABLE IV. Theoretical (H_n^{th}) and experimental [$H_n^{\text{expt}}(A)$] hyperfine fields for Cu-Mn (units: kG).

Shell	H_n^{th}	$H_n^{\text{expt}}(A)$	$\Delta K_n/K$[a]	Peak	Expt. assign.
1	−43.9	−50.9±1.0	−9.83±0.2	*A*	1
2	+12.0	+7.62±0.21	1.47±0.04	*M*	2
3	+2.7	+3.0±0.16	0.58±0.03	*N*	3
4	−12.4	−10.3±0.21	−1.98±0.04	*B*	4
5	−0.2	−2.7±0.21	−0.52±0.04	*C*	5
6	−0.6				
≥7		+1.8±0.12	+0.34±0.02	*P*	7

[a]Reference 13.

TABLE V. Theoretical (H_n^{th}) and experiment [$H_n^{expt}(A)$] hyperfine fields for Cu-Fe (units: kG).

Shell	H_n^{th}	$H_n^{expt}(A)$	$\Delta K_n/K$[a]	Peak	Expt. assign.
1	−36.4	−37.7±2.2	−5.24±0.3	*A*	1
2	+19.0	+14.0±0.2	+1.85±0.03	*M*	2
3	+1.5	+2.1±0.2	0.28±0.03	*N*	5
4	−9.9	−9.1±0.2	−1.20±0.03	*B*	3
5	+0.6				
6	+0.6				
≥7		−2.7±0.2	−0.36±0.02	*C*	4

[a]References 15 and 16.

calculated hyperfine fields. $H_n^{expt}(A)$ and $H_n^{expt}(B)$ are the fields estimated from the experimental Knight-shift data $\Delta K_n/K$ using either method *A*, Eq. (11), or method *B*, Eq. (10). Also listed are the conventional nomenclature of the satellite peaks by capital letters and the assignment of these peaks to the different shell atoms as found in the literature. These assignments are in general based on the line shape, width, and relative intensities of the satellites obtained from spectra of powder samples. A more reliable identification of the satellites can be obtained from single-crystal measurements. Varying the orientation of the crystal relative to the external field results in line patterns which should in principle permit an unambiguous assignment of the satellites to the atomic shells. For some few cases, the experimental assignments listed in Tables II–VI are based on this more rigorous method.

Cu-V: For several reasons this system is very complicated. For instance, the V solubility is very small. The susceptibility is more or less temperature independent[9] indicating an extremely large Kondo temperature. This is not necessarily in contrast to the calculated local moment of $1.1\mu_B$ since for such small moments one expects large fluctuation effects. Follstaedt and Slichter[9] have detected two satellites *G* and *C*, showing an appreciable field dependence and assigned them to the 2nd (or the 4th) and to the 3rd shell. In addition a very large quadrupole split satellite is found which they assign to the first neighbor. In order to compare the measured Knight shifts of peaks *G* and *C* with our calculated H_n values we have used, somewhat arbitrarily, for method *A* a Kondo temperature $T_K=0$ and the calculated total moment of $1.3\mu_B$. For method *B* we used the measured susceptibility[10] and again $1.3\mu_B$ for the moment. Due to the uncertainty of the susceptibility only the ratio H_2/H_3 is actually meaningful to compare. Our calculated values are in reasonable agreement with the measured $\Delta K_n/K$ values and therefore support the assignment of peak *G* and *C* to the 2nd and 3rd shell.

Cu-Cr: This system has been carefully studied by two groups.[11,12] From the Knight shift values of Aton *et al.*[11] we estimated the hyperfine fields $H_n^{expt}(A)$ by using the measured spin value $S=1.56$ which agrees well with our calculated total moment $3.33\mu_B$. The values H_n^{expt} are from saturation measurements below the Kondo temperature of 3 K.[12] The calculated values for the first, third, and fourth shell agree quite well with the measurements and the identification of Aton *et al.* The assignment of the satellite peaks *C*, *P*, and *N* is very unclear according to these authors. From our calculations and the clear trends shown in Figs. 1 and 2 we can exclude that peak *P* refers to the second neighbor. Since it does not fit to other calculated fields either we conclude that it should arise from a shell further away than the sixth one. The identification of peak *C* as the fifth shell is compatible with our results.

Cu-Mn: This system has been carefully studed by Aton, Stakelon, and Slichter[13] and others.[14] The measured Knight-shift parameters $\Delta K_n/K$ are listed in Table IV. Using this information together with method *A* of Sec. II and the experimental value $S=2.0$ for the total spin (our calculated value derived from the total moment of Table I is 1.8) we have evaluated the hyperfine fields $H_n^{expt}(A)$. The agreement between experimental and theoretical data is very good, clearly confirming the

TABLE VI. Theoretical (H_n^{th}) and experimental [$H_n^{expt}(A)$,$H_n^{expt}(B)$] hyperfine fields for Cu-Co (units: kG).

Shell	H_n^{th}	$H_n^{expt}(A)$	$H_n^{expt}(B)$	$\Delta K_n/K$[a]	Peak	Expt. assign.
1	−13.7	−14.8±0.1	−6.3	−1.38±0.01		
2	+10.8	+8.0±0.1	+3.4	+0.74±0.01	*M*	2
3	+0.3					
4	−3.4	−3.0±1	−1.3	−0.28±0.01	*B*	3 or 4
5	+0.5					
6	+0.6					

[a]References 16 and 17.

identification of the peaks for the first four shells. In view of the smallness of our calculated value for the fifth shell the assignment of peak C to the fifth shell is questionable.

Cu-Fe: From the experimental Knight-shift data of Boyce and Slichter[15] as well as Stakelon and Slichter[16] we have estimated the hyperfine field values $H_n^{\text{expt}}(A)$ using the experimentally determined total spin value of $S=1.25$ which agrees with our value in Table I. The Kondo temperature is $T_K=29$ K. The agreement between theory and experiment is quite good for the very large negative field of the first shell and the large positive field of the second shell. However, serious disagreement occurs for the assignments of the satellites B and N. From the very smooth trends shown in Figs. 1 and 2, especially for the third and fourth shell, the assignment of peak B to the third shell is inconceivable. If correct, it would also question the assignments of the third and fourth shells for all adjacent impurities, for which we get good agreement with the experiments. Our data clearly suggest that peak B refers to the fourth shell. Moreover peak N fits better to the third shell, instead of the fifth one. Finally peak C, which has been assigned to the fourth shell,[15] should belong to a shell further away than the sixth one.

As mentioned above, most experimental assignments are to some degree uncertain because they are based only on powder measurements. That even single crystal investigations do not necessarily give the correct assignments can be seen in the case of satellite B. Although the line patterns with their number of lines and relative intensities of peak B for various crystal orientations seem to be in agreement with the expectations for the third atomic shell,[16] this identification is in contradiction with several other findings: The relative intensity of peak B to peak M from powder patterns is found to be around 2.2 (Ref. 15) instead of 4, but in agreement with our new assignment requiring a factor 2. The data for the anisotropic Knight-shift tensor deduced for satellite B from the single-crystal measurements are not able to account for the line shape of Alloul and Ishii's low-temperature powder measurements[17] in contrast to the data for satellite M.[17] Finally, in their simple model calculations, Cohen and Slichter[1] also find a problem with the assignment of satellite B. Their calculated anisotropic Knight-shift components for the third shell are not consistent with the experimental ones. Thus, although single-crystal measurements are without doubt the most powerful method to identify the origin of the various satellites, there still seems to remain some uncertainty.

Using our corrected assignments Fig. 1 and especially Fig. 2 show that these values fit excellently into the trends obtained for the adjacent impurities. The inherent correlation between the results for different impurities, which we obtain from our *ab initio* theory without any parameter adjustment, is the strongest argument in favor of our new assignment.

Cu-Co: The small moment of Co indicates that spin fluctuations should be important and a Curie-Weiss law should not be valid. Nevertheless the data $H_n^{\text{expt}}(A)$ were estimated from the measured $\Delta K_n/K$ data[16,18] by Eq. (11) with $T_K=0$ and $S=0.43$ (see Table I). For the data $H_n^{\text{expt}}(B)$ the measured susceptibility of Tournier and Blandin[19] ($\chi=4\times10^{-27}$ emu/mol) and the moment of Table I has been used. In both cases considerable uncertainty in the susceptibility exists so that only the ratios of the hyperfine fields for different shells should be compared. There is quite good agreement and from our data we can rigorously assign peak B to the fourth shell.

Cu-Ni and Cu-Ti: According to our calculations Ni and Ti impurities are nonmagntic in Cu. Experimentally also in these cases NMR satellites are found. They could be calculated by applying a constant magnetic field which would induce a moment on the Ni and Ti impurities which itself would be the origin of the magnetization oscillations. From the regular behavior found in Fig. 2 for the ratios H_n/M_0 of the magnetic impurities it is tempting to extrapolate these curves to the adjacent nonmagnetic impurities Ti and Ni for which (without external field) both H_n and M_0 vanish. Contrary in an external field small fields H_n and a local moment M_0 are induced, being in strength proportional to the external field. Preliminary calculations show that the above speculation seems to be justified. For simplicity we apply in the calculation a small magnetic field only on the impurity and on four neighboring Cu shells. For the case of a Ni impurity we obtain a relatively large negative field for the first shell and an equally large but positive field for the second shell. The corresponding ratios $\Delta H_1/M_0=-15.5$ and $\Delta H_2/M_0=+26.3$ (kGμ_B^{-1}) are just about what one expects by extrapolating the curves in Fig. 1. While the negative first-neighbor field is confirmed experimentally,[16] a positive field for the second neighbor has not been reported. For a Ti impurity we obtain a small, but positive field for the first shell and a much larger negative field for the second shell [$\Delta H_1/M_0=+4.4$, $\Delta H_2/M_0=-21.5$ (kGμ_B^{-1})]. The surprising result, that the field of the second shell is strongly negative and much larger than the one of the first shell, has already been speculated in the literature,[20] however, no firm conclusion has been reached.

IV. SUMMARY AND CONCLUSION

Based on density-functional theory and the Korringa-Kohn-Rostoker- (KKR) Green's function method we have self-consistently calculated the electronic structure of $3d$ impurities in Cu. Our attention has been focused on the induced magnetization polarization around the impurities. In particular we calculated the hyperfine fields for six shells of neighboring Cu atoms. By considering the hyperfine fields H_n for the different shells n as a function of the impurity charge, we find some very simple trends being characteristic for a given shell. Physically these are due to a spatial shift of the magnetization oscillations as a function of the impurity nuclear charge. In practically all cases we find good agreement with the measured Knight-shift satellite data. The agreement is, however, not completely quantitative. This might be partly due to uncertainties in the experimental impurity susceptibilities, partly due to the neglect of lattice relaxations and relativistic effects in the calculations. In most cases we can confirm the experimental assignments of the

satellite peaks to the different shell atoms around the impurities. In some cases, noticeably for the satellite *B* of Cu-Fe, we can correct erroneous assignments.

Summarizing we notice that density-functional theory gives a completely consistent picture not only for the local moments of the impurities[2,3] but also for the magnetization polarization of the host atoms. This is not a trivial result. It is well known that due to the local-density approximation density-functional theory has the character of a mean-field theory, and is not able to describe such important features as the Kondo effect or spin fluctuations. Nevertheless our results demonstrate that the impurity moments and the host polarization can reliably be calculated by the local-density-functional theory.

In this paper we have only calculated the Fermi-contact contribution to the hyperfine fields. Additional dipolar and orbital contributions exist and lead to an anisotropic Knight-shift tensor which can be obtained from single-crystal measurements. Since quite a few experimental data about the anisotropy exist it would be interesting to calculate also these terms in order to see whether an even more complete picture of the host polarization can be obtained.

ACKNOWLEDGMENTS

We thank S. Blügel and M. Weinert for their cooperation in the hyperfine field calculations, S. Blügel especially for implementing the Broyden acceleration method into the impurity code. The calculations were performed on the CRAY-X/MP computers under the auspices of the Höchstleistungsrechenzentrum (HLRZ) and the KFA Jülich.

[1]J. D. Cohen and C. P. Slichter, Phys. Rev. **22**, 45 (1980).
[2]R. Zeller, R. Podloucky, and P. H. Dederichs, Z. Phys. B **38**, 165 (1980); R. Podloucky, R. Zeller, and P. H. Dederichs, Phys. Rev. B **22**, 5777 (1980).
[3]P. J. Braspenning, R. Zeller, A. Lodder, and P. H. Dederichs, Phys. Rev. B **29**, 703 (1984).
[4]U. von Barth and L. Hedin, J. Phys. C **5**, 1629 (1972).
[5]V. L. Moruzzi, J. F. Janak, and A. R. Williams, *Calculated Electronic Properties of Metals* (Pergamon, New York, 1978).
[6]R. Zeller, J. Deutz, and P. H. Dederichs, Solid State Commun. **44**, 993 (1982).
[7]S. Blügel, H. Akai, R. Zeller, and P. H. Dederichs, Phys. Rev. B **35**, 3271 (1987).
[8]J. Deutz, R. Zeller, and P. H. Dederichs, Kernforschungsanlage Jülich Report Jül-1805, 1982.
[9]D. M. Follstaedt and C. P. Slichter, Phys. Rev. B **16**, 21 (1977).
[10]W. D. Weiss, Z. Metallkd. **58**, 895 (1967).
[11]T. J. Aton, T. S. Stakelon, and C. P. Slichter, Phys. Rev. B **21**, 4060 (1980).
[12]L. J. Azevedo, D. Follstaedt, and A. Narath, J. Appl. Phys. **50**, 1746 (1979).
[13]T. J. Aton, T. S. Stakelon, and C. P. Slichter, Phys. Rev. B **18**, 3337 (1978).
[14]N. Karnezos and J. Gardner, Phys. Rev. B **9**, 3106 (1974).
[15]J. B. Boyce and C. P. Slichter, Phys. Rev. B **13**, 379 (1976).
[16]T. S. Stakelon and C. P. Slichter, Phys. Rev. B **14**, 3793 (1976).
[17]H. Alloul and H. Ishii, J. Phys. (Paris) Lett. **38**, 449 (1977).
[18]D. V. Lang, D. C. Lo, J. B. Boyce, and C. P. Slichter, Phys. Rev. B **9**, 3077 (1974).
[19]R. Tournier and A. Blandin, Phys. Rev. Lett. **24**, 397 (1970).
[20]D. M. Follstaedt, D. Abbas, T. S. Stakelon, and C. P. Slichter, Phys. Rev. B **14**, 47 (1976).